



RESEARCH PAPER

 OPEN ACCESS  Check for updates

The BAX-binding protein MOAP1 associates with LC3 and promotes closure of the phagophore

Hao-Chun Chang ^a, Ran N. Tao^a, Chong Teik Tan ^a, Ya Jun Wu^b, Boon Huat Bay^b, and Victor C. Yu ^a

^aDepartment of Pharmacy, Faculty of Science, National University of Singapore, Singapore, Singapore; ^bDepartment of Anatomy, Yong Loo Lin School of Medicine, National University of Singapore, Singapore, Singapore

ABSTRACT

MOAP1 (modulator of apoptosis 1) is a BAX-binding protein tightly regulated by the ubiquitin-proteasome system. Apoptotic stimuli stabilize MOAP1 protein and facilitate its interaction with BAX to promote apoptosis. Here we show that in contrast to being resistant to apoptotic stimuli, MOAP1-deficient cells are hypersensitive to cell death mediated by starvation rendered by EBSS treatment. MOAP1-deficient cells exhibited impairment in macroautophagy/autophagy signaling induced by EBSS. Mechanistic analysis revealed that MOAP1-deficient cells had no notable defect in the recruitment of the pre-autophagosomal phosphatidylinositol-3-phosphate (PtdIns3P)-binding proteins, ZFYVE1/DFCP1 and WIPI2, nor in the LC3 lipidation mechanism regulated by the ATG12–ATG5–ATG16L1 complex upon EBSS treatment. Interestingly, MOAP1 is required for facilitating efficient closure of phagophore in the EBSS-treated cells. Analysis of LC3-positive membrane structures using Halo-tagged LC3 autophagosome completion assay showed that predominantly unclosed phagophore rather than closed autophagosome was present in the EBSS-treated MOAP1-deficient cells. The autophagy substrate SQSTM1/p62, which is normally contained within the enclosed autophagosome under EBSS condition, was also highly sensitive to degradation by proteinase K in the absence of MOAP1. MOAP1 binds LC3 and the binding is critically dependent on a LC3-interacting region (LIR) motif detected at its N-terminal region. Re-expression of MOAP1, but not its LC3-binding defective mutant, MOAP1-LIR, in the MOAP1-deficient cells, restored EBSS-induced autophagy. Together, these observations suggest that MOAP1 serves a distinct role in facilitating autophagy through interacting with LC3 to promote efficient phagophore closure during starvation.

Abbreviations: CQ: Chloroquine; EBSS: Earle's Balanced Salt Solution; GABARAP: Gamma-Amino Butyric Acid Receptor Associated Protein; IF: Immunofluorescence; IP: Immunoprecipitation; LAMP1: Lysosomal-Associated Membrane Protein 1; LIR: LC3-Interacting Region; MAP1LC3/LC3: Microtubule Associated Protein 1 Light Chain 3; MEF: Mouse Embryonic Fibroblast; MOAP1: Modulator of Apoptosis 1; PE: Phosphatidylethanolamine; PtdIns3K: class III PtdIns3K complex I; PtdIns3P: Phosphatidylinositol-3-phosphate; STX17: Syntaxin 17; ULK1: unc-51 like autophagy activating kinase 1.

ARTICLE HISTORY



Received 6 May 2020
Revised 16 February 2021
Accepted 22 February 2021


KEYWORDS

Autophagosome formation; autophagy; cell death; LC3-binding protein; LIR motif; nutrient deprivation

Macroautophagy, herein referred to as autophagy, is a highly conserved cellular process that was initially identified as a survival mechanism during nutrient-deprivation condition in yeast [1,2]. The process involves the formation of autophagosome that engulfs cytosolic molecules and organelles which are subsequently delivered to lysosome for degradation [3,4]. Autophagy can be classified into three distinct phases: recruitment of initiation complexes, nucleation and expansion of the phagophore membrane, followed by maturation of autophagosome through fusion with the lysosome that results in degradation of the substrates within the autolysosome structures [3]. In mammalian cells, upon autophagy initiation, the ULK1–ATG13–RB1CC1/FIP200–ATG101 complex and ATG9A protein will be recruited to nascent sites for initiating the process of formation of autophagosome by activating the class III PtdIns3K complex I (PtdIns3K) to induce the nucleation of the autophagosomal precursor, known as the

phagophore [5]. The PtdIns3K complex, which consists of the class III PtdIns3K, PIK3C3/VPS34, BECN1/Beclin 1, ATG14, AMBRA1, NRBF2 and PIK3R4/p115, activates local production of phosphatidylinositol-3-phosphate (PtdIns3P) at specific ER site known as the omegasome. PtdIns3P subsequently recruits effector proteins WIPI2 and ZFYVE1 to the omegasome via their PtdIns3P-binding domains. WIPI2, which is known to directly bind to ATG16L1, recruits the ATG12–ATG5–ATG16L1 complex to facilitate the elongation of phagophore [6]. Expansion of phagophore membrane requires the activation of the ubiquitin-like conjugation pathways to activate the orthologs of Atg8-family proteins, MAP1LC3/LC3 (microtubule associated protein 1 light chain 3) and GABARAP (GABA type A receptor-associated protein) [3]. The LC3 and GABARAP proteins will first be cleaved by ATG4B, which is a cysteine protease [7,8], and then further processed by the E1-like ubiquitin activating

CONTACT Victor C. Yu  phayuv@nus.edu.sg  Department of Pharmacy, Faculty of Science, National University of Singapore, 18 Science Drive 4, Singapore, 117543, Singapore

 Supplemental data for this article can be accessed [here](#).

© 2021 The Author(s). Published by Informa UK Limited, trading as Taylor & Francis Group.
This is an Open Access article distributed under the terms of the Creative Commons Attribution-NonCommercial-NoDerivatives License (<http://creativecommons.org/licenses/by-nc-nd/4.0/>), which permits non-commercial re-use, distribution, and reproduction in any medium, provided the original work is properly cited, and is not altered, transformed, or built upon in any way.

enzyme, ATG7, before being transferred to the E2-like ubiquitin conjugating enzyme, ATG3, followed by the conjugation of phosphatidylethanolamine (PE) through the E3-like ATG12-ATG5-ATG16L1 complex [9–13]. Interestingly, recent studies have suggested that in mammals, this Atg8-family protein conjugation system which converts LC3 (LC3-I) into the lipidated form (LC3-II) that makes up the autophagosomal membranes is also critical for the completion of the autophagosome [14–17].

MOAP1 is a BAX-associated protein enriched at outer mitochondria membrane that serves to facilitate BAX-dependent mitochondrial outer membrane permeabilization and apoptosis [18–20]. MOAP1 protein is ubiquitously expressed in low abundance in most tissues and cell types as it is highly regulated by the ubiquitin-proteasome system [21–23]. Apoptotic stimuli stabilize MOAP1 protein by inhibiting its poly-ubiquitination process during the early phase of apoptosis signaling. Although MOAP1 plays a critical role in facilitating BAX-mediated apoptosis, *moap1*^{-/-} mice do not exhibit notable developmental defect and are fertile [24]. Further analysis, however, revealed that *moap1*^{-/-} mice are remarkably resistant to hepatocellular apoptosis and lethality triggered by *in vivo* activation of the FAS signaling. Upon activation of FAS signaling, the BH3 protein BID will be cleaved by CASP8 to generate the active, truncated form of BID (tBID). tBID will then be targeted to mitochondria by interacting with MTCH2 at the outer mitochondrial membrane which is an essential step for tBID to promote mitochondrial outer membrane permeabilization and result in the release of apoptogenic factors such as cytochrome *c* from mitochondria [25]. Interestingly, tBID fails to interact with MTCH2 nor induce mitochondrial apoptosis signaling in the absence of MOAP1 and further analysis reveals that MOAP1 interacts with MTCH2 to activate its mitochondrial receptor function for tBID [24].

The *moap1*^{-/-} mouse embryonic fibroblasts (MEFs) are modestly resistant to apoptotic stimuli [18–20]. In this study, interestingly, *moap1*^{-/-} MEFs were found to be hypersensitive to cell death mediated by the nutrient deprivation paradigm, EBSS. As EBSS treatment is known to be a potent trigger of autophagy, hypersensitivity to cell death in the absence of MOAP1 may suggest that MOAP1-deficient cells are defective in mounting the survival defense mechanism by activating autophagy signaling. Indeed, similar hypersensitivity phenotype could also be seen in cells with defective autophagy signaling or suppression of autophagy signaling by chemical inhibitor. MOAP1-deficient cells and tissues showed impairment in autophagy. While MOAP1 did not appear to be required for the early steps of autophagy signaling, MOAP1 deficiency resulted in inefficient closure of phagophore which is required for maturation of autophagosome. Interestingly, a distinct LIR motif residing at the N-terminus region of MOAP1 was identified to be critically required for mediating its interaction with LC3 and facilitating phagophore membrane closure. Based on these observations, we propose that MOAP1 is a novel regulator of autophagy signaling that through binding to LC3 to

facilitate efficient closure of phagophore during autophagosome formation.

Results

MOAP1-deficient cells are hypersensitive to cell death mediated by nutrient deprivation condition rendered by EBSS treatment

MOAP1-deficient MEFs are resistant to apoptotic stimuli including staurosporine, etoposide and actinomycin D (Fig. S1A) [24]. To extend the investigation of potential roles of MOAP1 in regulating cell death mediated by non-apoptotic mechanism, we subjected the *Moap1*^{+/+} and *moap1*^{-/-} MEFs to an assortment of stress-related insults including proteolytic (MG132 or PS341), oxidative stress (H₂O₂ or As₂O₃) and nutrient deprivation paradigms, glucose/serum deprivation and EBSS treatment. Interestingly, while *moap1*^{-/-} MEFs were modestly resistant to cell death mediated by a variety of stress stimuli, they were hypersensitive to the starvation-mediated cell death rendered by EBSS treatment (Figure 1A and S1A). *MOAP1*^{-/-} HeLa cells, which were generated using the CRISPR-Cas9 gene editing system, displayed similar phenotype as the *moap1*^{-/-} MEFs (Figure 1B). Restoration of MOAP1 expression in the MOAP1-deficient HeLa cells by transient transfection was able to abolish the hypersensitivity to cell death phenotype mediated by EBSS treatment (Figure 1C).

To evaluate possible role of apoptosis signaling contributing to the cell death mediated by EBSS, *Moap1*^{+/+} and *moap1*^{-/-} MEFs were pre-treated with a pan caspase inhibitor, Q-VD-OPh (QVD), to block apoptotic cell death before subjecting the cells to EBSS treatment. While QVD was effective in inhibiting cell death triggered by etoposide (Fig. S1B, left panel), it failed to block the cell death mediated by the EBSS treatment (Fig. S1B, right panel). As nutrient deprivation condition mediated by EBSS is known to be a potent activator of autophagy [26], we then compared the cell death responses mediated by the EBSS treatment between the *moap1*^{-/-} and *atg5*^{-/-} MEFs. *atg5*^{-/-} MEFs are known to be defective in autophagy as ATG5 is one of the essential proteins for mediating autophagy signaling [13,27]. Indeed, *moap1*^{-/-} and *atg5*^{-/-} MEFs displayed similar heightened sensitivity phenotype to cell death mediated by the EBSS treatment (Figure 1D). To further validate the hypersensitivity phenotype observed in the MOAP1-deficient MEFs is associated with a defect in autophagy signaling, the lysosomal inhibitor chloroquine (CQ), which is a commonly used autophagy inhibitor, was added prior to EBSS treatment in the *Moap1*^{+/+} and *moap1*^{-/-} MEFs. While *Moap1*^{+/+} MEFs became more sensitive to EBSS-mediated cell death with CQ co-treatment, *moap1*^{-/-} MEFs exhibited similar degree of sensitivity to EBSS-mediated cell death with or without CQ co-treatment (Figure 1E).

MOAP1-deficient cells are defective in autophagy signaling

The processing of the LC3-I into lipidated form, LC3-II, which makes up the pre-autophagosomal membranes known

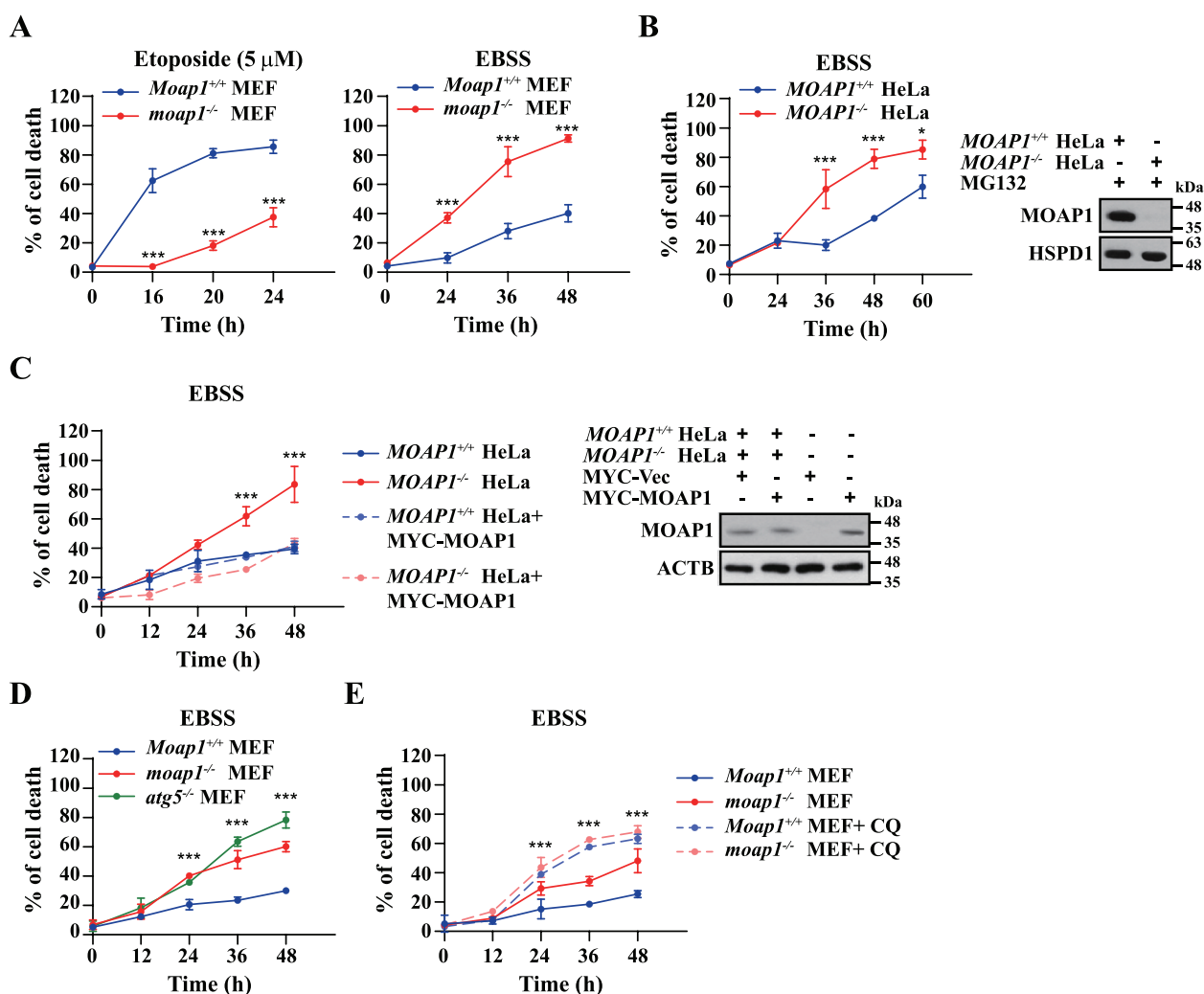


Figure 1. MOAP1-deficient cells are resistant to apoptotic cell death, but hypersensitive to cell death mediated by nutrient deprivation. (A) Cell death responses of the *Moap1*^{+/+} and *moap1*^{-/-} MEFs to etoposide and nutrient deprivation mediated by EBSS. At the indicated time points, cells were harvested and stained with propidium iodide (PI) before subjecting to FACS for cell death analysis. ****p* < 0.001 (Student's *t* test). (B) *MOAP1*-deficient HeLa cells displays hypersensitivity to cell death triggered by EBSS treatment. The *MOAP1*^{+/+} and *MOAP1*^{-/-} HeLa cells were subjected to EBSS treatment and cell death analysis was performed at the indicated time points (left panel). MG132 effectively upregulated MOAP1 in the *MOAP1*^{+/+} HeLa cells (right panel). **p* < 0.05, ****p* < 0.001 (Student's *t* test). (C) Transient re-expression of MOAP1 in the *MOAP1*-deficient HeLa cells abolishes the heightened cell death response to EBSS treatment. MOAP1 was expressed by transient transfection of plasmid encoding MYC-MOAP1 for 24 h in the *MOAP1*^{-/-} HeLa cells before subjecting to EBSS treatment. Cell death analysis at the indicated time points was performed using PI exclusion assay (left panel). MYC-tagged MOAP1 was expressed in the *MOAP1*^{-/-} HeLa cells to a similar level as endogenous MOAP1 in the *MOAP1*^{+/+} HeLa cells (right panel). ****p* < 0.001 (Student's *t* test). (D) MEFs that are defective in autophagy signaling display similar hypersensitivity phenotype to EBSS-mediated cell death as the *MOAP1*-deficient MEFs. ATG5-deficient MEFs were harvested at the indicated time points for cell death analysis as described in (A). ****p* < 0.001 (Student's *t* test). (E) Inhibition of autophagy signaling in MEFs by chloroquine confers similar heightened sensitivity phenotype to EBSS-mediated cell death as observed in the *MOAP1*-deficient MEFs. MEFs were treated with CQ (100 μ M) for 30 min before subjecting to EBSS treatment. Cells were harvested at the indicated time points for cell death analysis as described in (A). ****p* < 0.001 (Student's *t* test).

as phagophore, is an important step for the formation of autophagosome [28]. Indeed, conversion of LC3-I to LC3-II is widely used as a marker for estimating autophagic activity [29]. In mammalian cells, LC3B is generally thought to be the key player among all other Atg8-family protein isoforms for mediating starvation-induced autophagy signaling [30]. In addition to levels of LC3B-I and LC3B-II, SQSTM1, an autophagy receptor that recognizes ubiquitinated proteins or other cargo and deliver them for clearance through the autophagy-lysosome pathway, is also commonly used to monitor autophagic flux as its protein levels will be subjected to clearance by autophagy mechanism [29]. To begin the investigation into possible role of MOAP1 in regulating autophagy, levels of LC3 lipidation and clearance of SQSTM1 as an autophagic

substrate under the starvation condition mediated by EBSS treatment were subjected to western analysis. While levels of LC3-II were indistinguishable between the *Moap1*^{+/+} and *moap1*^{-/-} MEFs, clearance of SQSTM1 was significantly reduced in the *moap1*^{-/-} cells (Figure 2A and S2A). Similarly, reduction in the clearance of SQSTM1 was also observed in the *MOAP1*^{-/-} HeLa cells treated with the MTORC1 inhibitor, rapamycin, which is a known potent activator of autophagy signaling (Fig. S2B). Likewise, in comparison to the *Moap1*^{+/+} mice, clearance of SQSTM1 in liver, brain and muscle tissues of the *moap1*^{-/-} mice subjected to fasting for 24 h was also reduced (Figure 2B and S2C). However, with 48 h of fasting, difference in the clearance of SQSTM1 in the livers was less pronounced between the *Moap1*^{+/+} and the *moap1*^{-/-} mice

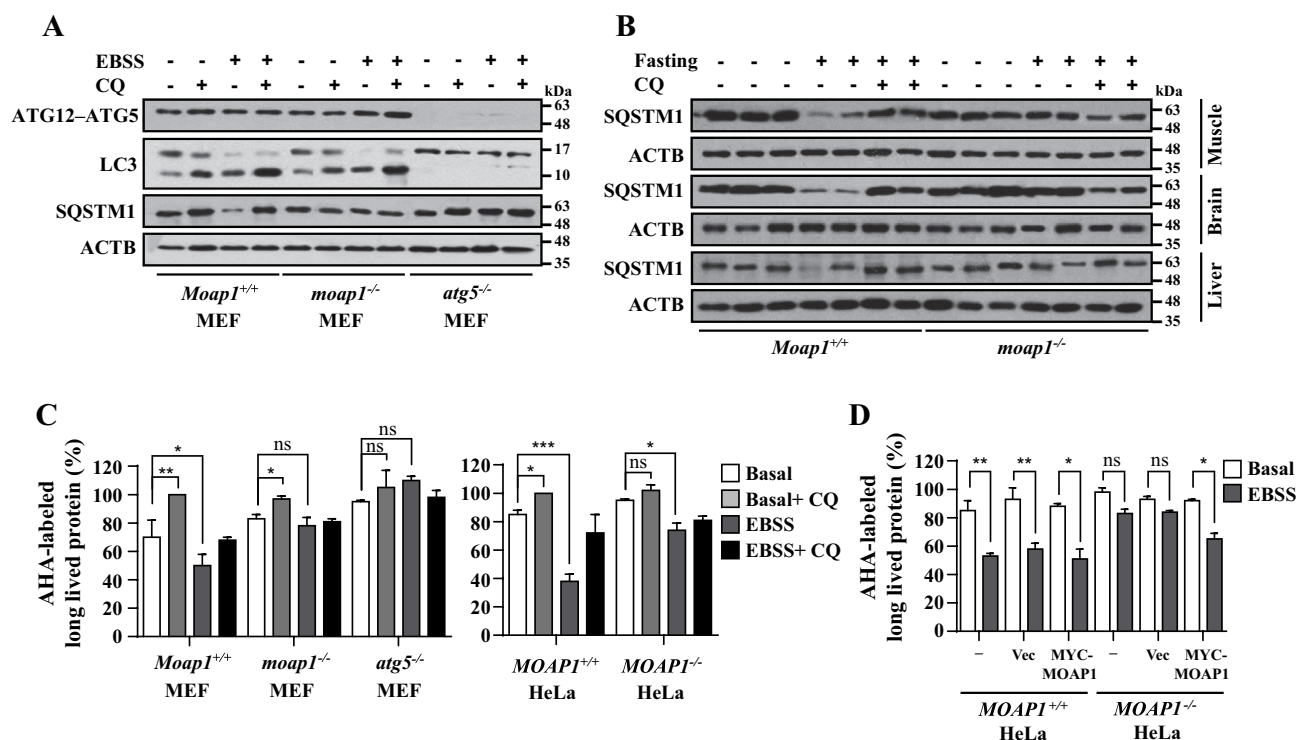


Figure 2. MOAP1-deficient cells are defective in autophagy. (A) Degradation of autophagy substrate SQSTM1 is suppressed in the absence of MOAP1. Total cell lysates were prepared from the *Moap1*^{+/+} and *moap1*^{-/-} MEFs after 6 h of EBSS treatment in the presence or absence of autophagy inhibitor CQ (100 μ M). Cell lysates were prepared for western analysis with the indicated antibodies. ATG12-ATG5 and LC3 were used as markers to monitor the activation of autophagy signaling. (B) Degradation of SQSTM1 is inhibited in multiple tissues in the *moap1*^{-/-} mice subjected to fasting. Autophagy inhibitor CQ was injected intraperitoneally at dose of 50 mg/kg of body weight. The *Moap1*^{+/+} and *moap1*^{-/-} mice were then subjected to fasting for further 24 h before being euthanized. Brain, liver and skeletal muscle from the mouse hind limb were isolated from the mice for preparation of total tissue lysates for western analysis. (C) Autophagy-mediated long-lived protein degradation is inhibited in the absence of MOAP1. The *Moap1*^{+/+}, *moap1*^{-/-} and *atg5*^{-/-} MEFs (left panel) were pre-labeled with AHA for 16 h before being subjected to EBSS treatment for further 6 h. The amount of long-lived proteins was analyzed using FACS. The experiment was also performed using the *MOAP1*^{+/+} and *MOAP1*^{-/-} HeLa cells (right panel). **p* < 0.05, ***p* < 0.01, ****p* < 0.001, ns, not significant (Student's *t* test). (D) The degradation defect of long-lived protein in the *MOAP1*^{-/-} HeLa cells is eliminated by re-expressing MOAP1. Plasmids encoding vector for control or MYC-MOAP1 were transiently transfected into the *MOAP1*^{-/-} HeLa cells. 24 h post-transfection, the cells were labeled with AHA for another 16 h as described in (C) before subjecting to 6 h of EBSS treatment, followed by cell harvesting for FACS analysis. **p* < 0.05, ***p* < 0.01, ns, not significant (Student's *t* test).

(Fig. S2C). To assess and compare autophagic activity activated by EBSS in the wild-type and MOAP1-deficient cells, we quantified the autophagy-dependent long-lived protein degradation between the *Moap1*^{+/+} and *moap1*^{-/-} MEFs under the starvation condition rendered by EBSS. We labeled all the long-lived protein substrates with an amino acid analog, L-azidohomoalanine (AHA) as previously described [31]. While the signal intensity of the AHA-labeled protein at basal level was reduced in the *Moap1*^{+/+} MEFs under 6 h of EBSS treatment, no reduction in signal intensity was seen in the *atg5*^{-/-} nor *moap1*^{-/-} MEFs (Figure 2C, left panel). Similar phenotype was also observed in the *MOAP1*^{-/-} HeLa cells (Figure 2C, right panel). The ability in the degradation of AHA-labeled protein in the MOAP1-deficient cells was restored by re-expressing MOAP1 transiently (Figure 2D).

MOAP1 is dispensable for the early steps of autophagy signaling involved in the initiation and elongation of phagophore

Upon autophagic induction, ULK1 and PtdIns3K complexes are activated to trigger the recruitment of the PtdIns3P-binding proteins ZFYVE1/DFCP1 and WIPI2 to the initiation sites for nucleation of phagophore [5]. WIPI2 recruits

ATG12-ATG5-ATG16L1 proteins to form a E3-like complex which is responsible for the LC3 lipidation and expansion of phagophore. To evaluate involvement of MOAP1 in regulating different phases of autophagosome formation, recruitment of ZFYVE1, WIPI2, ATG12, ATG5 and ATG16L1 to sites of phagophore nucleation and elongation, which are visually appearing as puncta [29], was evaluated in the *MOAP1*^{+/+} and *MOAP1*^{-/-} HeLa cells. Generation of PtdIns3K complexes, which are labeled by EGFP-2X FVYE tag, and the formation of ZFYVE1 or WIPI2 puncta were examined in the *MOAP1*^{+/+} and *MOAP1*^{-/-} HeLa cells subjected to EBSS treatment. No noticeable difference was noted in the PtdIns3P generation as well as formation of ZFYVE1 or WIPI2 puncta between the *MOAP1*^{+/+} and *MOAP1*^{-/-} cells at 5 and 15 min post-EBSS treatment (Fig. S3A-C). Similarly, ATG12, ATG5, ATG16L1 and p-ATG16L1, which is the phosphorylated and activated form of ATG16L1, were also able to form puncta-like structures in an indistinguishable manner between the *MOAP1*^{+/+} and *MOAP1*^{-/-} cells (Figure 3A, B and S3D). Furthermore, p-ATG16L1 was found to be in close proximity with ATG12-ATG5 complex in both the *MOAP1*^{+/+} and *MOAP1*^{-/-} cells during starvation mediated by EBSS treatment (Figure 3C). Similarly, the assembly of the ATG12-ATG5-ATG16L1 complex was also not affected in the absence of MOAP1 (Figure

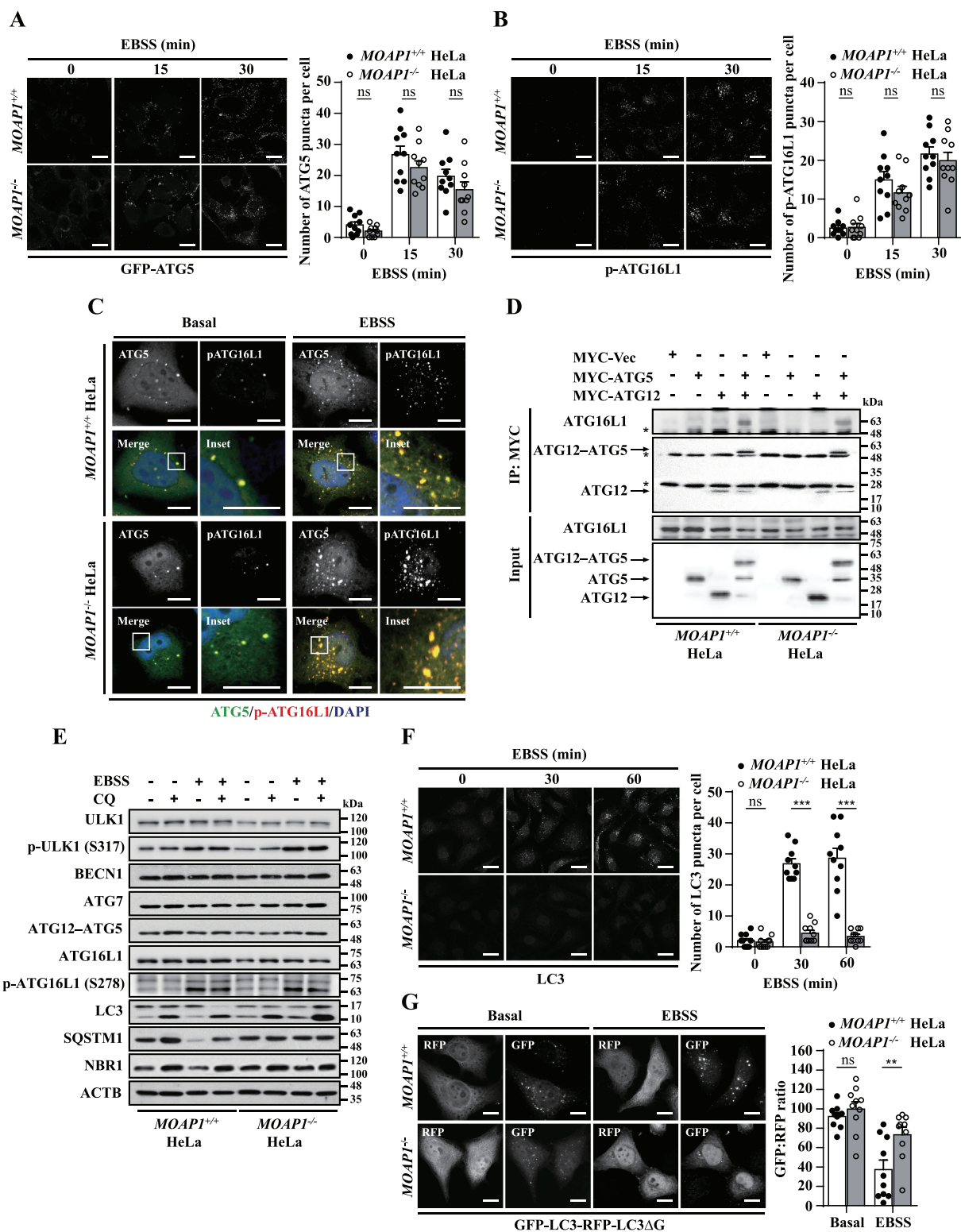


Figure 3. MOAP1 is dispensable during the early steps of autophagy signaling involving initiation and elongation of phagophore. (A and B) Formation of ATG5 or p-ATG16L1 puncta is unaffected in the absence of MOAP1 in cells treated with EBSS. The *MOAP1*^{+/+} and *MOAP1*^{-/-} cells were subjected to EBSS treatment for the indicated time periods. The cells were then harvested for immunofluorescence staining by detecting the presence of GFP-ATG5 (A) or p-ATG16L1 puncta (labeled with Cy3) (B) to monitor the formation process of autophagosome during autophagy signaling. Scale bar: 10 μ m. ns, not significant (Student's *t* test). (C) Loss of MOAP1 does not affect conjugation of ATG12-ATG5-ATG16L1 complex. The *MOAP1*^{+/+} and *MOAP1*^{-/-} HeLa cells were harvested under basal condition or after 2 h of EBSS treatment before being subjected to immunofluorescence staining. GFP-ATG5 or Cy3 labeled-p-ATG16L1 puncta were used as markers for detecting the formation of ATG5-12-16 L1 complex. Scale bar: 5 μ m. (D) Loss of MOAP1 does not affect the interaction between ATG5-12 and ATG16L1 complex. Plasmid encoding MYC-ATG5 or ATG12 was transfected into the *MOAP1*^{+/+} or *MOAP1*^{-/-} HeLa cells. After 24 h, the transfected cells were subjected to immunoprecipitation to evaluate the interaction between ATG16L1 and ATG12-ATG5. Arrows: indicated protein signal; Asterisk: IgG signal. (E) LC3 conjugation process induced by EBSS treatment is unaffected by the absence of MOAP1. Total cell lysates from the *MOAP1*^{+/+} and *MOAP1*^{-/-} HeLa cells were harvested after 6 h of EBSS treatment. BECN1, ATG7, ATG5-12 and LC3 are the markers for the upstream signaling events during autophagic induction whereas SQSTM1 and NBR1 are the autophagy substrates. (F) Low number of LC3 puncta in the MOAP1-deficient EBSS-treated cells. The *MOAP1*^{+/+} and *MOAP1*^{-/-} HeLa cells were subjected to EBSS treatment for 30 or 60 min as indicated. At the indicated time points, the treated and untreated *MOAP1*^{+/+} or *MOAP1*^{-/-} cells were subjected to immunofluorescence staining. The number of LC3

puncta was then quantified by ImageJ analysis. Scale bar: 10 μ m. *** $p < 0.001$, ns, not significant (Student's t test). (G) Low level of autophagy flux in the absence of MOAP1 during starvation. The *MOAP1*^{+/+} and *MOAP1*^{-/-} HeLa cells were transfected with plasmid encoding the GFP-LC3-RFP-LC3G reporter prior to EBSS treatment for 2 h. The level of fluorescence signals was then measured and the ratio of GFP:RFP was then calculated by FACS analysis. Scale bar: 5 μ m. ** $p < 0.01$, ns, not significant (Student's t test).

3D). Western analysis also revealed that the levels of the regulatory proteins including ULK1, BECN1, ATG7, ATG5 remained unaltered in the *MOAP1*^{-/-} cells, while clearance of SQSTM1 upon activation of autophagy by EBSS was markedly inhibited (Figure 3E).

While the lipidated LC3 (LC3-II) was at similar levels in the lysates prepared from the EBSS-treated *MOAP1*^{+/+} or *MOAP1*^{-/-} cells (Figures 2A and Figures 3E), the number of LC3 puncta associated with endogenous or GFP-tagged LC3, which are regarded as a marker for estimating abundance of autophagosome, appeared in markedly lower quantity in the *MOAP1*^{-/-} cells (Figure 3F and S3E). As autophagosome is thought to exist in transient state because of its ability to rapidly fuse with lysosome for degradation, it remained a possibility that significantly lower number of LC3 puncta observed in the *MOAP1*^{-/-} cells could be caused by an acceleration of autophagy flux. To evaluate this possibility, plasmid encoding the GFP-LC3-RFP-LC3G was transfected into the *MOAP1*^{+/+} and *MOAP1*^{-/-} HeLa cells to permit estimation of the autophagic flux by measuring the rate of ATG4 cleavage of LC3 into LC3-I and the turnover of LC3 protein, as previously described [32]. Upon expression, GFP-LC3-RFP-LC3G would first be cleaved by ATG4 into GFP-LC3 and RFP-LC3G in equimolar ratio. While the GFP-LC3 will undergo normal lipidation and lysosomal degradation, RFP-LC3G, which lacks the amino acid required for lipidation, would not be lipidated by the ATG12-ATG5-ATG16L1 complex and would remain in the cytosol, thereby serving as an internal control (Figure 3G). The ratios of GFP and RFP fluorescence signals in the *MOAP1*^{+/+} and *MOAP1*^{-/-} HeLa cells subjected to EBSS treatment were determined by direct epifluorescence and FACS analysis. In contrast to the *MOAP1*^{+/+} cells where a dramatic reduction was observed in the GFP:RFP ratio following EBSS treatment, only a modest decrease was detected in the EBSS-treated *MOAP1*^{-/-} HeLa cells, suggesting a decrease rather than an increase in autophagy flux in the absence of MOAP1 (Figure 3G).

MOAP1 is required for promoting closure of phagophore

The low number of LC3-positive puncta detected by immunofluorescence (IF) (Figure 3F and S3E) albeit comparable level of LC3-II in western analysis in the EBSS-treated MOAP1-deficient cells (Figure 3E) suggest that the LC3-II may not be membrane-bound or its attachment to membrane might be weaker in the absence of MOAP1. To evaluate this possibility, we next studied the membrane association characteristics of LC3-II in the *MOAP1*^{+/+} and *MOAP1*^{-/-} cells using membrane fractionation and extraction analysis. Similar to the *MOAP1*^{+/+} cells, LC3-II was found to be predominantly associated with membrane in the *MOAP1*^{-/-} cells under the starvation condition (Fig. S4A). To evaluate whether membrane association characteristics of LC3-II

during starvation would be qualitatively different between the *MOAP1*^{+/+} and *MOAP1*^{-/-} cells, we compared several lysis buffers containing varying strength of detergents, from relatively strong detergents such as RIPA and Triton X-100, to milder condition such as digitonin and 0.1 M sodium carbonate [33], for their abilities in extracting LC3-II out from the membrane fractions of the *MOAP1*^{+/+} and *MOAP1*^{-/-} cells subjected to EBSS treatment. No difference was noted in the membrane association characteristics of LC3-II between the *MOAP1*^{+/+} and *MOAP1*^{-/-} cells based on the lysis buffers tested (Fig. S4B).

To investigate further the distribution of LC3 and the state of the LC3-positive membrane structures, we deployed the recently described HaloTag-LC3 autophagosome completion assay for differentiating unclosed phagophore and closed autophagosome. First, Halo-tagged LC3 was stably expressed in the *MOAP1*^{+/+} and *MOAP1*^{-/-} HeLa cells (Figure 4A). To permit differentiation of Halo-tagged LC3 localized at phagophore membrane versus enclosed autophagosome, the cells were first labeled with a saturated amount of the membrane-impermeable HaloTag ligand (MIL), followed by the membrane-permeable HaloTag ligand (MPL) as previously described [34]. In the *MOAP1*^{+/+} cells subjected to EBSS treatment, phagophore (MIL+, appearing in green), and closed autophagosome (MPL+, appearing in red), were robustly detected after 2 h of EBSS treatment (Figure 4B-D). In contrast, far fewer closed autophagosome was detected in the *MOAP1*^{-/-} cells subjected to EBSS treatment. Interestingly, Halo-LC3 signal associated with phagophore was readily detected in the MOAP1-deficient cells (Figure 4B-D). The marked reduction in the MPL+ closed autophagosome in the MOAP1-deficient cells is reminiscent of low number of LC3 puncta detected by IF staining of endogenous LC3 (Figure 3F). Thus, it seems likely that the LC3-positive membranes found in the closed autophagosome were more sensitive to detection by IF than those associated with phagophore, thereby resulting in poor signals in the form of LC3 puncta detected by IF in the MOAP1-deficient cells as they primarily harbor phagophore. To evaluate this possibility, we performed dual Halo and IF labeling of Halo-LC3 in *MOAP1*^{+/+} and *MOAP1*^{-/-} HeLa cells treated with EBSS. Indeed, only the MPL-positive autophagosome, but not the MIL-positive phagophore appeared to coalesce with the signals detected by the IF method in these cells (Fig. S4C), suggesting that the reduction of LC3 puncta in the *MOAP1*^{-/-} cells could in part cause by the low number of closed autophagosome present in the cells.

To evaluate the role of MOAP1 in promoting phagophore closure further, we assessed the degree of protection from proteinase digestion of the autophagy substrates, SQSTM1 and LC3 [15,35]. In the *MOAP1*^{+/+} cells, the SQSTM1 and LC3 in the lysates enriched with autophagosome prepared from the untreated cells were readily degraded by proteinase

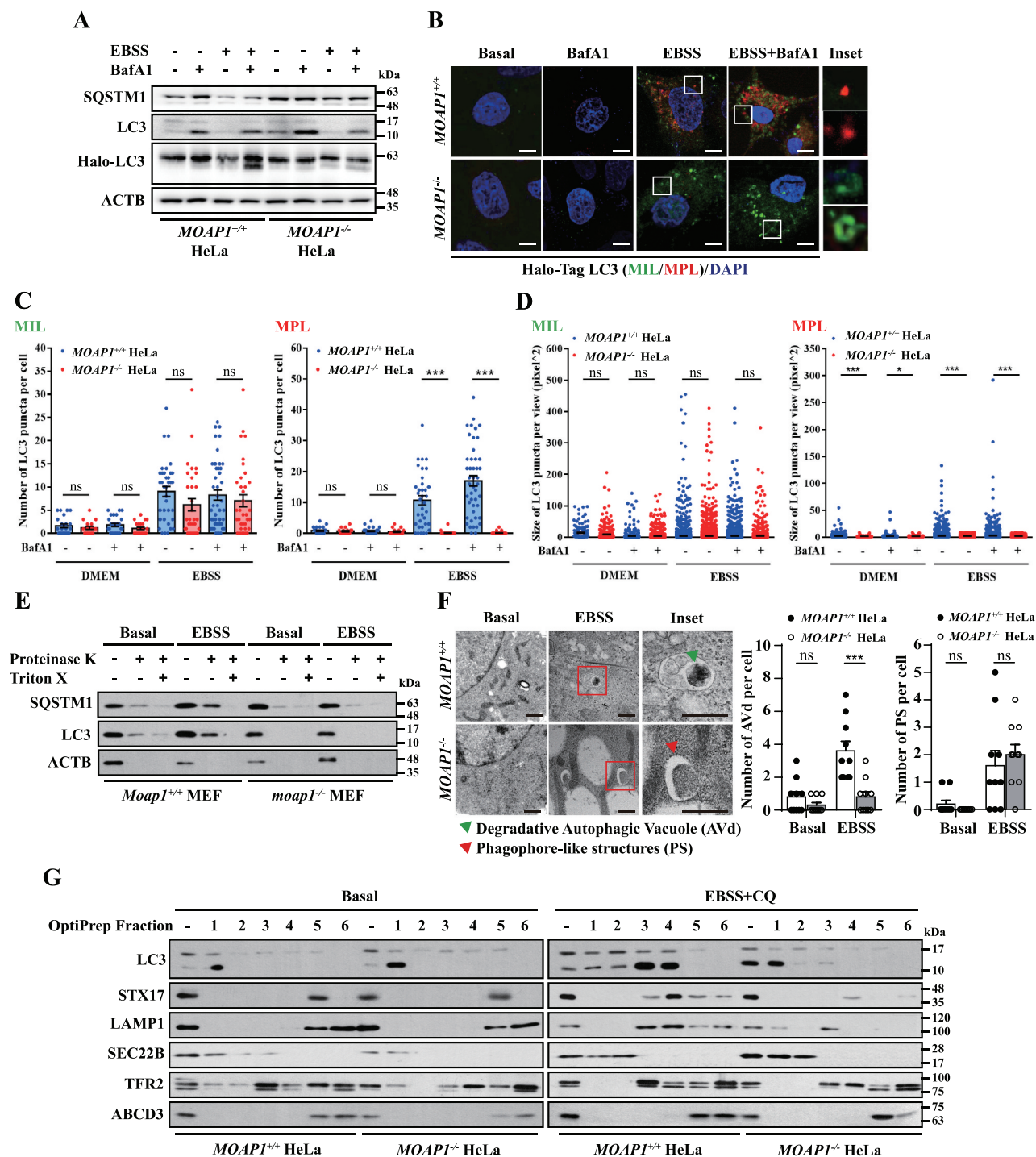


Figure 4. MOAP1 is required for promoting efficient closure of phagophore. (A) Establishment of the *MOAP1*^{+/+} and *MOAP1*^{-/-} HeLa cells stably expressing Halo-LC3. The *MOAP1*^{+/+} and *MOAP1*^{-/-} HeLa cells stably expressing Halo-LC3 were subjected to EBSS or EBSS plus BafA1 (100 nM) treatment for 3 h. Total cell lysates were then prepared for western analysis. SQSTM1 and LC3 was used as markers to validate the autophagy response of these cell lines. (B) Detection of LC3 in the phagophore membrane, but not autophagosome, in the *MOAP1*^{-/-} cells during starvation. The *MOAP1*^{+/+} and *MOAP1*^{-/-} HeLa cells stably expressing Halo-LC3 were subjected to EBSS or EBSS plus the autophagy inhibitor, BafA1, treatment for 3 h. The cells were then permeabilized with 20 μ M of digitonin for 3 min, followed by staining with MIL (Labeled in green) for 30 min. These cells were then fixed with 4% PFA, followed by staining with MPL (Labeled in red) for another 30 min as described. The representative images for the MIL/MPL-positive puncta were shown in the magnified images from the boxed area (Inset). Scale bar: 5 μ m. (C and D) Detection of MIL-positive, MPL-negative puncta in the *MOAP1*^{-/-} cells under EBSS treatment in the absence or presence of BafA1. The *MOAP1*^{+/+} and *MOAP1*^{-/-} HeLa cells stably expressing Halo-LC3 were subjected to EBSS or EBSS plus BafA1 treatment for 3 h as described above. The number (C) and size (D) of LC3 puncta labeled by different ligand (MIL or MPL) was calculated using ImageJ analysis. ****p* < 0.001, ns, not significant (Student's *t* test). (E) SQSTM1 and LC3 in the autophagosomal fraction isolated from the *MOAP1*-deficient cells are more sensitive to proteinase K-mediated degradation. Cell fraction enriched with autophagosomes from the EBSS-treated MEFs was isolated for proteinase K digestion. SQSTM1 and LC3 were significantly less protected from proteinase K digestion in the fraction prepared from the *MOAP1*^{-/-} HeLa cells. (F) Phagophore-like structures, but not autophagic vacuoles, were predominantly present in the *MOAP1*^{-/-} HeLa cells subjected to EBSS treatment. Autophagic vacuoles or phagophore-like structures formed upon EBSS treatment were visualized by EM. The vacuoles together with the degraded cargos were categorized as degradative autophagic vacuole (AVd, green arrowheads) whereas the unclosed membrane structure with no cargos inside were categorized as phagophore-like structure (PS, red arrowheads) (left panel). The number of these membrane structures detected in the *MOAP1*^{+/+} and *MOAP1*^{-/-} HeLa cells were then quantified (right panel). Scale bar: 200 nm. ****p* < 0.001, ns, not significant (Student's *t* test). (G) Absence of LC3 in the lysate fractions containing STX17 and LAMP1

prepared from the *MOAP1*^{-/-} HeLa cells subjected to EBSS treatment. The *MOAP1*^{+/+} and *MOAP1*^{-/-} HeLa cells were pre-treated with CQ for 30 min, followed by further co-treatment with EBSS and CQ for further 2 h before subjecting to membrane flotation assay using OptiPrep density gradient. LC3 represent the protein components on the phagophore membrane whereas STX17 and LAMP1 are markers to assess the maturation of autophagosome.

K, but they became partially resistant in the same lysates prepared from the EBSS-treated cells (Figure 4E) as some of the SQSTM1 and LC3 proteins were protected from proteinase K when they are contained within the enclosed autophagosome [15]. Indeed, in agreement with the findings from the Halo-LC3 experiments that EBSS-treated *MOAP1*^{-/-} are predominantly enriched with phagophore, but not autophagosome, SQSTM1 and LC3 in the autophagosome-enriched lysates prepared from the *MOAP1*^{-/-} cells were significantly more sensitive than those from the *MOAP1*^{+/+} cells to proteinase K digestion (Figure 4E).

Closure of phagophore is critical step for maturation of autophagosome into autolysosome through fusion with the lysosome. We next examined the autophagic vacuoles in the *MOAP1*^{+/+} and *MOAP1*^{-/-} cells subjected to EBSS treatment by electron microscopy (EM) analysis. Degradative autophagic vacuole-like structure, with the characteristics of being partially degraded, electron-dense contents were readily detected in the *MOAP1*^{+/+}, but not in the *MOAP1*^{-/-} cells (green arrowheads, Figure 4F). Instead, accumulation of empty vacuoles that resemble unclosed phagophore was more readily detected in the EBSS-treated *MOAP1*^{-/-} cells (red arrowheads, Figure 4F). To evaluate further on the role of MOAP1 in affecting the closure of phagophore, we examined the identity of the proteins in the fractions of cell lysates commonly associated proteins in phagophore and autophagosome by using the membrane flotation assay as previously described [36]. Cell homogenates from the EBSS-treated *MOAP1*^{+/+} and *MOAP1*^{-/-} cells were first subjected to differential centrifugation to separate the crude lysates containing various organelles into 1,000 x g (1 K), 3,000 x g (3 K), 25,000 x g (25 K) and 100,000 x g (100 K) fractions (Fig. S4D). The 25 K fraction, which is known to be enriched with autophagosome, was further separated into multiple fractions by density gradient ultracentrifugation using sucrose gradients, followed by 5 to 30% OptiPrep gradient, as previously described [36]. Upon EBSS treatment, LC3-II, which is thought to be derived from the ER, as marked by SEC22B, expanded from SEC22B-positive OptiPrep fractions 1–2 to fractions 3–6 containing LAMP1 (lysosomal associated membrane protein 1). Similarly, STX17 (syntaxin 17), a soluble N-ethylmaleimide-sensitive factor attachment protein receptor protein that is required for mediating the fusion of autophagosome with endosomes/lysosomes [37,38], was also found in the OptiPrep fractions 3–6 (Figure 4G). Loss of MOAP1 did not affect formation of other membrane structures such as endosome, as marked by TFR2 (Transferrin Receptor 2), or peroxisome, labeled by the ABCD3/PMP70 (ATP binding cassette subfamily D member 3) (Figure 4G). In contrast, although LC3-II could be detected in the OptiPrep fraction 1 that is enriched with SEC22B in the *MOAP1*^{-/-} cells, it was poorly detected in fractions 3–6. Likewise, STX17 and LAMP1 proteins were also found to be in low abundance in these fractions, suggesting that the LC3-II-positive fractions detected in the

EBSS-treated *MOAP1*^{-/-} cells did not correspond well to the fractions of proteins expected to be present in mature autophagosome (Figure 4G).

MOAP1 is a LC3-binding protein

Interestingly, three putative LIR motifs are noted in the primary amino acid sequence of MOAP1, suggesting that MOAP1 may be an LC3-interacting protein (Figure 5A). Indeed, endogenous MOAP1 associated with LC3-I or LC3-II robustly in HeLa cells. Interestingly, MOAP1-LC3-II interaction was enhanced further in the EBSS-treated cells (Figure 5B). MOAP1 appeared to localize in close proximity with LC3 in HeLa cells upon treatment with EBSS (Figure 5C). Mutagenesis analysis of the three putative LIR motifs in MOAP1 showed that only the LIR motif at its N-terminus, a.a. 49–52 (YRLI), is critically required for mediating its interaction with LC3 (Figure 5D, E). The MOAP1 mutant with point mutations in the LIR, through alanine substitution of the hydrophobic residues, Y49A/L52A, which is hereon referred to as MOAP1-LIR mutant (MOAP1-LIR), failed to interact with LC3. *In vitro* pull-down analysis also validated that MOAP1, but not MOAP1-LIR mutant, was able to bind to LC3 directly in a dose-dependent manner (Figure 5F). We then tested whether MOAP1 is able to interact with other Atg8-family protein isoforms including members of LC3 (LC3A, LC3B and LC3C) and GABARAP (GABARAP, GABARAPL1 and GABARAPL2) family of proteins. Among all the mammalian Atg8-family protein isoforms, MOAP1 was able to associate with all the LC3 family of proteins but not any of the GABARAP proteins (Fig. S5A, B).

The roles of MOAP1 in facilitating autophagy and apoptosis signaling appear separable

Although it is still not completely clear the basis by which LC3 puncta was only readily detectable by using Halo-tagged LC3 system, but not by conventional IF in the MOAP1-deficient EBSS-treated cells, it is nevertheless a unique phenotype associated with MOAP1 deficiency as re-expression of MOAP1, but not its LC3-binding defective mutant, MOAP1-LIR, in the *MOAP1*^{-/-} HeLa cells was able to restore the number of LC3 puncta detected using IF to a level similar to that in the *MOAP1*^{+/+} cells (Figure 6A). Similarly, the reduction in levels of long-lived protein mediated by autophagic degradation was partially reinstated in the *MOAP1*^{-/-} cells by re-expressing MOAP1, but not MOAP1-LIR (Figure 6B). Furthermore, unlike MOAP1, re-expressing MOAP1-LIR mutant in the *MOAP1*^{-/-} HeLa cells failed to confer protection to SQSTM1 and LC3 from proteinase K digestion, suggesting that the interaction between MOAP1 and LC3 is critical for facilitating closure of autophagosome (Figure 6C).

MOAP1 serves a critical role in mediating FAS-mediated apoptosis signaling in liver by binding to the outer mitochondrial membrane protein MTCH2 to activate its function as

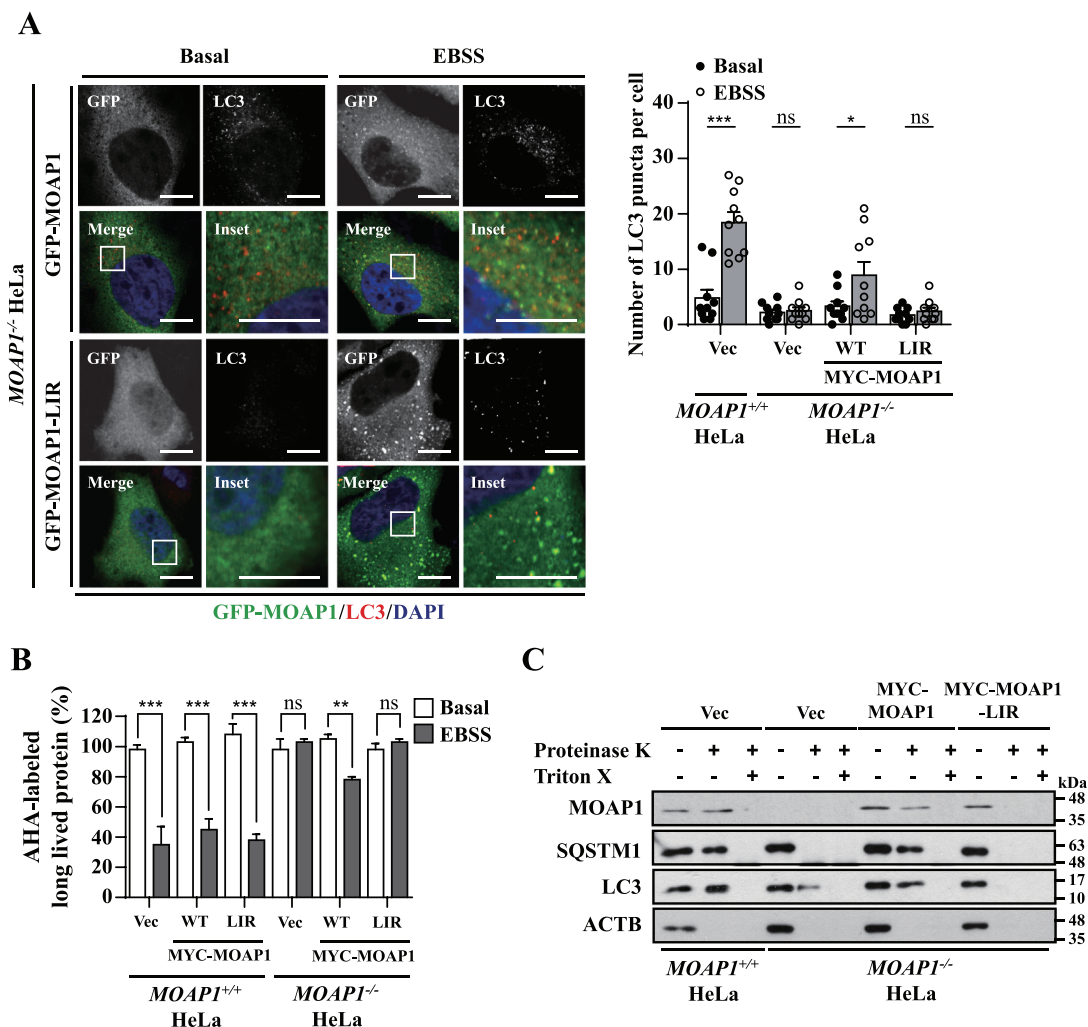


Figure 6. MOAP1-LC3 interaction is required for efficient execution of autophagy signaling. (A) MOAP1, but not its LC3-binding defective mutant, is able to restore the formation of LC3 puncta during autophagy signaling mediated by EBSS treatment. Plasmid encoding GFP-MOAP1 or its LC3-binding defective mutant, GFP-MOAP1-LIR, was transfected into *MOAP1*^{-/-} HeLa cells for 24 h prior to EBSS treatment. After 2 h of EBSS treatment, the cells were harvested for immunofluorescence analysis to visualize GFP-MOAP1 and LC3 (left panel). The number of LC3 puncta was quantified in the *MOAP1*^{+/+} and *MOAP1*^{-/-} HeLa cells re-expressing MOAP1 or MOAP1-LIR mutant. Scale bar: 5 μ m. * $p < 0.05$, *** $p < 0.001$, ns, not significant (Student's *t* test). (B) Restoration of autophagy flux in the *MOAP1*^{-/-} HeLa cells by re-expressing MOAP1, but not its LC3-binding defective mutant. Plasmid encoding MYC-MOAP1 or MOAP1-LIR mutant was co-transfected with plasmid encoding GFP-LC3-RFP-LC3 reporter into the *MOAP1*^{+/+} and *MOAP1*^{-/-} HeLa cells prior to EBSS treatment. The level of fluorescence signals was then measured and the ratio of GFP:RFP was then calculated by FACS analysis. ** $p < 0.01$, *** $p < 0.001$, ns, not significant (Student's *t* test). (C) Re-expression of MOAP1, but not its LIR mutant, in the *MOAP1*^{-/-} cells, confers protection of SQSTM1 and other autophagic substrates from proteinase K digestion. The *MOAP1*^{-/-} HeLa cells were transiently transfected with plasmid encoding MYC-MOAP1 or MOAP1-LIR mutant for 24 h prior to EBSS treatment. The cell fraction enriched with autophagosome was then isolated as described in (Figure 4E) for proteinase K digestion. MOAP1, but not its LIR mutant, restored the resistance of SQSTM1 and LC3 to degradation by proteinase K in the *MOAP1*^{-/-} HeLa cells.

mediated SQSTM1 clearance (Fig. S6C) and hypersensitivity to cell death phenotype induced by EBSS treatment (Fig. S6D). Together, these observations providing evidence to support the idea that the functions of MOAP1 in facilitating apoptosis and autophagy signaling are separable.

Discussion

Through analysis of potential role of MOAP1 in regulating multiple types of cell death, we uncovered a unique role of MOAP1 in facilitating autophagy signaling. In yeast, the conjugation of PE onto the C terminus of Atg8 through the ubiquitin-like systems is required for the formation of autophagosome [8,11]. Although LC3, which is an ortholog of Atg8, shares similar mechanism of the lipidation process in

mammalian cells, emerging evidence suggests that the absence of LC3 and its homolog GABARAP family member of proteins does not completely block the formation of autophagosome, but rather results in defective sealing of phagophore, which leads to a delay in the maturation of autophagosome [15,17]. Mizushima and colleagues reported that cells lacking the Atg3 PE conjugation system exhibit failure in the recruitment of STX17 to the autophagosome, as well as impaired degradation of the inner autophagosome membrane [17]. In a recent study, Deretic and colleagues suggested that the recruitment of STX17 to the autophagosome is critically dependent on LC3 and IRGM (immunity-related GTPase M) to form the autophagosome recognition particle (ARP) protein complex [39]. In this study, we showed that in the absence of MOAP1, closure of phagophore, but not initiation

or elongation of phagophore was affected. Although MOAP1 does not associate with STX17 or LAMP1 directly (Fig. S5C), it may be possible that MOAP1 is part of the ARP complex to facilitate the interaction of LC3 and STX17. Moreover, CHMP2A has recently been identified as a critical regulator for promoting closure of phagophore, while its depletion leads to accumulation of phagophore, CHMP2A does not seem to be required for the recruitment of STX17 to LC3-positive structures [34]. MOAP1-deficient cells have far fewer closed autophagosome under EBSS conditions. However, in contrast to CHMP2A depletion, we did not observe a significant increase in the level of phagophore in the *MOAP1*^{-/-} cells treated with EBSS, suggesting perhaps other regulatory mechanisms such as negative feedback loop may have a role in regulating the homeostatic levels of phagophore.

Although apoptosis and autophagy signaling are initially thought of as functionally distinct pathways for cells to respond to multiple stress signals under different physiological contexts [40], increasing evidence suggests that many proteins involved in apoptosis also have distinct role in regulating autophagy signaling. For example, members of the BCL2 family of proteins have also been reported to participate in regulating autophagy. BCL2 and MCL1 are known as anti-apoptotic proteins that antagonize BAX and BAK1 [41]. BECN1, an ortholog of yeast Vps30/Atg6 that interacts with Vps34 and Vps15 in the autophagy initiation complex, was also found to interact with and is inhibited by BCL2 and MCL1 via its BH3-only domain [42,43]. Hence, the interaction between BECN1 and these BCL2 proteins may play an important role in determining whether the cells undergo autophagy or apoptosis under different cellular or physiological contexts [44,45]. SH3GLB1/Bif-1/endophilin B1, which was originally discovered by its ability to interact with BAX to activate its conformational change [46], was also found to participate in the formation of autophagosome by interacting with BECN1 and UVRAG under nutrient deprivation condition [47]. While MOAP1 has been demonstrated to be a critical mediator of mitochondria-dependent apoptosis signaling, our current study uncovers a distinct role of MOAP1 in the autophagy signaling process. Interestingly, re-expressing the apoptosis-defective mutant of MOAP1, MOAP1^{L120E}, was competent to rescue the autophagy-deficient phenotype in the MOAP1-deficient cells under EBSS treatment (Fig. S6B, C), raising the possibility that the roles of MOAP1 in regulating apoptosis and autophagy signaling are potentially separable. Nevertheless, further work would be necessary to evaluate possible role of MOAP1 in participating in possible crosstalk between autophagy and apoptosis signaling.

During autophagy signaling, the cytosolic form of LC3 is first cleaved by ATG4 to form LC3-I which exposes its c-terminal glycine residue for lipid conjugation to form LC3-II. The membrane-associated lipidated LC3 can then be visualized as LC3 puncta by IF staining and this observation is generally accepted as a marker for estimating robustness of autophagy activity [29]. Interestingly, in this study, we observed a difference in LC3 puncta detection using conventional IF versus Halo-tag labeling system in the MOAP1-deficient cells subjected to EBSS treatment. It appears that

the phagophore membrane-associated LC3-II presented in the *MOAP1*^{-/-} cells was poorly detected by IF, but can be easily detected using the Halo-tagged LC3 labeling system (Figures 3E and Figures 4B). As LC3-II in the wildtype and MOAP1-deficient cells are both membrane-bound and share similar membrane association characteristics under a range of extraction conditions tested, it seems that the LC3-II in the phagophore of MOAP1-deficient cells could be in conformation or distribution that affects its sensitivity to be detected by IF, thereby contributing the poor LC3 signals in IF. Since MOAP1 associates with LC3 and the interaction was shown to be further enhanced under EBSS treatment (Figure 5B), it seems possible that conformation of the phagophore membrane bound LC3 was affected in the absence of interaction with MOAP1. Interestingly, with the Halo-LC3 system, we were able to readily detect the presence of LC3-associated phagophore, but relative few closed autophagosome in the MOAP1-deficient cells (Figure 4B).

Most, if not all, mice deficient in any of the ATG family of proteins that is essential for the initiation of autophagy or elongation of phagophore would exhibit severe developmental defects [27]. While MOAP1 plays a role in facilitating efficient closure of phagophore via a LC3-dependent mechanism (Figure 4), *in vivo* analysis, however, showed that a reduction in the rate of SQSTM1 degradation was significantly less affected in tissues of mice subjected to 48 h rather than 24 h of fasting (Fig. S2C), suggesting that MOAP1 deficiency may result in a delay rather than blockage of autophagy signaling. It is also possible that in the *in vivo* setting, there are effective compensatory mechanism to counteract the deficiency caused by the absence of MOAP1. In the recent study published by Lazarou and colleagues which revealed that among all the mammalian Atg8-family protein homologs, LC3B, as well as all the other LC3 family of proteins, are not essential for regulating the starvation-induced autophagy signaling [15]. Since MOAP1 appears to interact specifically with LC3 but not GABARAP proteins, it may also potentially explain why the mice developed normally. To permit better understanding of the role of MOAP1 in regulating autophagy signaling *in vivo*, it is necessary to conduct additional experiments in complex cellular and tissue contexts in future.

Materials and methods

Animals

All the animal experiments were performed under the regulation and review of Institutional Animal Care and Use Committee of National University of Singapore. Generation of *moap1*^{-/-} mice was described previously [24]. *Moap1*^{+/+} and *moap1*^{-/-} mice were derived from the same *moap1*[±] founders in the C57/BL6 background and were in-bred for less than six generations. Genotyping of animals used in the experiments were conducted routinely. Mice were weaned at 21 day old and maintained on the normal Chow diet at 0700–1900 h light cycle and

controlled temperature and humidity environment. Only male mice were used for all experiments in this study.

Antibodies

The primary antibodies used were as follows: ACTB (Sigma-Aldrich, SAB5500001), ATG16L1 (Abcam, ab187671), ATG16L1 (phospho-S278; Abcam, ab192542), ATG5 (nanoTools, 0262-100), ATG7 (Abcam, ab133528), BECN1 (Cell Signaling Technology, 3495), cl-CASP3 (Cleaved-Asp175; Cell Signaling Technology, 9661), FLAG (Sigma-Aldrich, F3165), GST (Santa Cruz Biotechnology, sc-138), HA (Abcam, ab9110), His (Santa Cruz Biotechnology, clone H-3), HSPD1/HSP60 (Santa Cruz Biotechnology, sc-13115), LMNA/lamin A/C (Santa Cruz Biotechnology, sc-376248), LAMP1 (Cell Signaling Technology, 9091), LC3B (Cell Signaling Technology, 2775), MOAP1 (Sigma-Aldrich, HPA000939), MYC (Santa Cruz Biotechnology, sc-40), NBR1 (Novus Biologicals, H00004077-M01), SQSTM1/p62 (Abcam, ab56416), ABCD3/PMP70 (Abcam, ab109448), SEC22B (Abcam, 181076), STX17 (MBL International, PM076), TFR2 (Abcam, 185550), TOMM20 (Santa Cruz Biotechnology, sc-11415), TUBA/tubulin (Santa Cruz Biotechnology, sc-8035), ULK1 (Cell Signaling Technology, 8054), ULK1 (phospho-S317; Cell Signaling Technology, 12753), WIPI2 (Abcam, ab105459).

Cell cultures

HEK293T (ATCC, CRL-11268), MEF and HeLa (ATCC, CRM-CCL-2) cells were cultured in Dulbecco's Modified Eagle's Medium (DMEM; Sigma-Aldrich, D1152) supplemented with 10% fetal bovine serum (FBS; Sigma-Aldrich, F7524), 3.7 g/L sodium bicarbonate (Sigma-Aldrich, S5761), 1% sodium pyruvate (Sigma-Aldrich, S8636) and 1% penicillin-streptomycin (Sigma-Aldrich, P4333) and maintained in 37°C, 5% CO₂ incubator (Thermo Forma Series 2). Cells were treated with different drugs or cultured under EBSS (Thermo Scientific, 24010043) where indicated. For experiments that required blocking the lysosome activity under EBSS-mediated autophagy signaling activation, cells were pre-treated with chloroquine (CQ, 50 mg/ml; Sigma-Aldrich, C6628) or bafilomycin A₁ (BafA1, 100 nM; Sigma-Aldrich, SML1661) for 30 min, followed by co-treatment with EBSS and CQ-BafA1 for further period of times as indicated. For the overexpression experiments, cells were transfected using polyethylenimine (PEI; Sigma-Aldrich, 408727) or ViaFectTM (Promega, E4981) following the manufacturer's instruction and subjected to other treatment after 24 h to 48 h later.

Constructs

For mammalian expression, cDNAs encoding ATG5, LAMP1 (human), LC3B (human), MOAP1 (human full-length or the indicated mutants), MTCH2 (human) and STX17 (human) were cloned into the pXJ-40 expression vector (Life Science Market, PVT20255). pBMN HA-GBRP, pMX-IY HA-GBRPL1 and pMX-IY HA-GBRPL2 was a gift from Michael

Lazarou (Addgene, 89296, 89297 and 89298) [15]. pEGFP-2xYFVE was a gift from Harald Stenmark (Addgene, 140047) [48]. pX330-U6-Chimeric_BB-CBh-hSpCas9 was a gift from Dr Feng Zhang (Addgene, 42230) [49]. pMRX-IP-GFP-LC3-RFP-LC3ΔG was a gift from Dr. Noboru Mizushima (Addgene, 84572) [32].

Immunoprecipitation

Total cell lysate was harvested by scraping cells in 1 ml of IP lysis buffer (50 mM HEPES, pH 7.9 [Sigma-Aldrich, PHG0001], 250 mM NaCl [Sigma-Aldrich, S3014], 5 mM Ethylenediaminetetraacetic acid [EDTA; Sigma-Aldrich, E6758], 1% NP-40 [Abcam, ab142227], 1% Triton X-100 [Sigma-Aldrich, T8787]) containing complete Pierce Proteinase Inhibitor (Thermo Scientific, A32963). Samples were collected and placed on ice for 30 min before centrifugation at 20,000 × g for 12 min. 1 ml of supernatant from each sample was incubated with anti-MYC antibody for 4 h. After incubation with the antibody, protein A agarose beads (Sigma-Aldrich, PROTAA-RO) were added into the lysate and incubated at 4°C overnight. The beads were collected by centrifuging at 1,500 × g for 1 minute and washed with 1 ml IP lysis buffer for 6 times and eluted with 2X sample buffer.

Immunofluorescence staining

MEF or HeLa cells were seeded on coverslips and fixed in 4% v:v paraformaldehyde (Sigma-Aldrich, P6148) in PBS for 13 min and permeabilized in 0.1% v:v Triton X-100 in PBST for 10 min at room temperature. Samples were blocked with 3% bovine serum albumin (BSA; Sigma-Aldrich, A9418) v:v PBST for 1 h at room temperature and incubated with specific primary antibody (1:250) diluted in 3% BSA for 1 h at room temperature. After washing three times with PBST for 15 min, samples were incubated with secondary antibodies (Life Technology) conjugated to indicate fluorophore (1:500) for 1 h at room temperature. Samples were washed three times and mounted in Dako fluorescence mounting medium (Agilent, S3023) on slides for confocal microscopy imaging. All images were acquired from the Olympus Fluoview FV10i confocal microscopy (60X oil objective).

Duolink proximity ligation assay

The Duolink[®] In Situ Red starter kit mouse/rabbit (Sigma-Aldrich, DUO92101) was used to perform the proximity ligation assay. Briefly, HeLa cells were seeded on coverslip and transiently transfected with HA-MOAP1 (human full-length MOAP1 or the indicated mutants) and MYC-LC3 for 24 h. Cells were fixed in 4% paraformaldehyde for 10 min and permeabilized in 0.1% v:v Triton X-100 in PBST for 10 min at room temperature. Samples were blocked with 3% BSA v:v PBST for 1 h at room temperature and incubated with anti-MYC and anti-HA at 1:200 dilution (in 3% BSA) for 1 h at room temperature. Samples were then washed and incubated with the PLA probes and ligated, amplified, mounted for confocal microscopy (Olympus FV10i).

PI exclusion assay

For cell death analysis, cells were harvested after drug treatment and stained with fluorochrome solution (RNaseA 0.5 mg/mL [Sigma-Aldrich, R6513], 50 µg/mL propidium iodide [PI; Sigma-Aldrich, P4170] in PBS) at 37°C for 30 min. For apoptosis analysis, cells were harvested after drug treatment and stained using a FITC Annexin V Apoptosis Detection Kit II (BD Biosciences, 556570) in accordance with the manufacturer's protocol. Flow cytometry via Beckman Coulter CytoFLEX flow cytometer with CytExpert 2.1 software was used to measure cell death and apoptosis assays.

Transmission electron microscopy

Cells grown in the Lab-Tek II chamber slide (Thermo Scientific™, 154941) were fixed with 5% glutaraldehyde (Sigma-Aldrich, G5582) for 2 h at 4°C and washed with PBS for three times and proceeded for dehydration. Dehydration was performed in graded concentration of ethanol (Sigma-Aldrich, 1.07017) from 25%, 50%, 75%, 95% to 100% for 10 min and a final 10 min incubation with 100% acetone (Sigma-Aldrich, 179124). Cells are infiltrated in 100% acetone:resin (1:6) overnight at room temperature and incubated at 80°C oven for 4 h. The embedded cells were trimmed, sectioned, and imaged by TEM (JEOL 1400FLASH TEM).

AHA long-lived protein labeling

50 M of the L-methionine analog L-azidohomoalanine (AHA; Invitrogen, C10289) was added into the medium for 18 h to label the newly synthesized proteins. After labeling, the medium was removed and replaced with regular DMEM containing 2 mM L-methionine (Sigma-Aldrich, M5308) for 2 h to chase out the short-lived proteins. To detect the amount of AHA labeled proteins, the cells were harvested and subjected to the Click-iT reaction (a chemo-selective ligation reaction between an azide and an alkyne). A reaction mix of TAMRA alkyne (Invitrogen, T10183), 1 mM TCEP (Sigma-Aldrich, C4706), 100 M TBTA (Sigma-Aldrich, 678937) and 1 mM CuSO₄ (Sigma-Aldrich, 451657) was added to resuspend the cell pellet after trypsinized the cells. The reaction mixture was then incubated at room temperature for 2 h in the dark and subjected to FACS analysis as previously described [31].

Proteinase K protection assay

The cells were harvested in the homogenization buffer containing 20 mM HEPES, pH 7.6, 220 mM mannitol (Sigma-Aldrich, M9647), 70 mM sucrose (Sigma-Aldrich, S0389) and 1 mM of EDTA. After centrifugation at 500 x g at 4°C for 5 min, the samples were treated with mock, 25 µg/ml proteinase K (Thermo Scientific, EO0491) alone and proteinase K plus 0.2% Triton X-100 for 10 min on ice, separately. The reactions were stopped by adding 1 mM of Phenylmethanesulfonyl fluoride (PMSF; Sigma-Aldrich, P7626) for another 10 min on ice. The samples were then subjected to trichloroacetic acid (TCA; Sigma-Aldrich,

T6399) precipitation and resuspended in 2X sample buffer for western analysis as previously described [15].

Autophagosome membrane flotation assay

The cells were harvested in the sucrose resuspension buffer containing 20 mM HEPES, pH 7.6, 220 mM mannitol, 400 mM sucrose and 1 mM of EDTA. The homogenates were subjected to sequential differential centrifugation at 1,000 x g for 10 min, 3,000 x g for 10 min, 25,000 x g for 20 min and 120,000 x g for 2 h. The middle fraction which contained the autophagosomes were then suspended in OptiPrep gradient buffer (Sigma-Aldrich, D1556) ranging from 0 to 30% density of OptiPrep resuspended in 20 mM Tricine-KOH, pH 7.4 (Sigma-Aldrich, T5816), 40 mM sucrose and 1 mM EDTA. The centrifugation was performed at 150,000 x g for 3 h and each fraction was collected for western analysis as previously described [36].

HaloTag-LC3 Autophagosome completion assay

Cells stably expressing Halo-LC3 were subjected to different treatment as indicated. The cells were stained with 1 M MIL (Promega, G1001) at 37°C for 15 min. The cells were then fixed with 4% paraformaldehyde at 37°C for 5 min. After wash the fixed cells with PBS for three times, the cells were stained with 1M MPL (Promega, G8251) at 37°C for 30 min. After that, the samples were washed three times and mounted in Dako anti-fade mounting medium (Agilent, S3023) on slides for confocal microscopy imaging. All images were acquired from the Olympus Fluoview FV3000 confocal microscopy (100 X oil objective). The number and size of the MIL/MPL-positive puncta were analyzed using Image J software (NIH). Confocal images of the color channels of MPL and MIL were first inverted and converted into binary mode. Quantification of the number and size of MIL and MPL puncta was performed using the "Analyze Particles" function and normalized to the number of nuclei to derive the number per cell. The size of the MIL/MPL structures was calculated based on their area in pixel.

Statistical analysis

All statistical data are expressed as mean ± standard error of mean, unless otherwise stated. ImageJ software is used to analyze confocal images and quantify protein levels from western blot images. *p < 0.05, **p < 0.01, ***p < 0.001 (Student's t-test).

Acknowledgments

We thank Dr Noboru Mizushima for providing the inducible *atg5^{-/-}* cell line and Dr Shen Han-Ming for providing the EGFP-LC3 stable expressing cell line and technical support for establishing the AHA protein labeling system. We thank Drs Shen Han-Ming, Lim Kah Leong and Liou Yih Cherng for valuable technical advices.

Disclosure statement

No potential conflict of interest was reported by the authors.

Funding

This research is supported by grants awarded to VCY by the Singapore Ministry of Health's National Medical Research Council under its OF-IRG scheme (NMRC/OFIRG/0011/2016), the Singapore Ministry of Education Academic Research Fund Tier 1 (R-148-000-288-114) and the NUSMed-FoS Joint Research Program on Healthy Brain Aging (R-148-000-280-133).

ORCID

Hao-Chun Chang  <http://orcid.org/0000-0003-2705-0027>

Chong Teik Tan  <http://orcid.org/0000-0002-9503-8364>

Victor C. Yu  <http://orcid.org/0000-0003-3270-4734>

References

- [1] Takeshige K, Baba M, Tsuboi S, et al. Autophagy in yeast demonstrated with proteinase-deficient mutants and conditions for its induction. *J Cell Biol.* 1992 Oct;119(2):301–311. PubMed PMID: 1400575; PubMed Central PMCID: PMCPMC2289660.
- [2] Tsukada M, Ohsumi Y. Isolation and characterization of autophagy-defective mutants of *Saccharomyces cerevisiae*. *FEBS Lett.* 1993 Oct 25;333(1–2):169–174. PubMed PMID: 8224160.
- [3] Kroemer G, Marino G, Levine B. Autophagy and the integrated stress response. *Mol Cell.* 2010 Oct 22;40(2):280–293. PubMed PMID: 20965422; PubMed Central PMCID: PMCPMC3127250.
- [4] Mizushima N, Yoshimori T, Ohsumi Y. The role of Atg proteins in autophagosome formation. *Annu Rev Cell Dev Biol.* 2011;27:107–132. PubMed PMID: 21801009.
- [5] Dikic I, Elazar Z. Mechanism and medical implications of mammalian autophagy. *Nat Rev Mol Cell Biol.* 2018 Jun;19(6):349–364. PubMed PMID: 29618831.
- [6] Dooley HC, Razi M, Polson HE, et al. WIPI2 links LC3 conjugation with PI3P, autophagosome formation, and pathogen clearance by recruiting Atg12-5-16L1. *Mol Cell.* 2014 Jul 17;55(2):238–252. PubMed PMID: 24954904; PubMed Central PMCID: PMCPMC4104028.
- [7] Hemelaar J, Lelyveld VS, Kessler BM, et al. A single protease, Apg4B, is specific for the autophagy-related ubiquitin-like proteins GATE-16, MAP1-LC3, GABARAP, and Apg8L. *J Biol Chem.* 2003 Dec 19;278(51):51841–51850. PubMed PMID: 14530254.
- [8] Tanida I, Ueno T, Kominami E. LC3 conjugation system in mammalian autophagy. *Int J Biochem Cell Biol.* 2004 Dec;36(12):2503–2518. PubMed PMID: 15325588.
- [9] Fujita N, Itoh T, Omori H, et al. The Atg16L complex specifies the site of LC3 lipidation for membrane biogenesis in autophagy. *Mol Biol Cell.* 2008 May;19(5):2092–2100. PubMed PMID: 18321988; PubMed Central PMCID: PMCPMC2366860.
- [10] Glick D, Barth S, Macleod KF. Autophagy: cellular and molecular mechanisms. *J Pathol.* 2010 May;221(1):3–12. PubMed PMID: 20225336; PubMed Central PMCID: PMCPMC2990190.
- [11] Ichimura Y, Kirisako T, Takao T, et al. A ubiquitin-like system mediates protein lipidation. *Nature.* 2000 Nov 23;408(6811):488–492. PubMed PMID: 11100732.
- [12] Kaur J, Debnath J. Autophagy at the crossroads of catabolism and anabolism. *Nat Rev Mol Cell Biol.* 2015 Aug;16(8):461–472. PubMed PMID: 26177004.
- [13] Mizushima N, Noda T, Yoshimori T, et al. A protein conjugation system essential for autophagy. *Nature.* 1998 Sep 24;395(6700):395–398. PubMed PMID: 9759731.
- [14] Kaufmann A, Beier V, Franquelim HG, et al. Molecular mechanism of autophagic membrane-scaffold assembly and disassembly. *Cell.* 2014 Jan 30;156(3):469–481. PubMed PMID: 24485455.
- [15] Nguyen TN, Padman BS, Usher J, et al. Atg8 family LC3/GABARAP proteins are crucial for autophagosome-lysosome fusion but not autophagosome formation during PINK1/Parkin mitophagy and starvation. *J Cell Biol.* 2016 Dec 19;215(6):857–874. PubMed PMID: 27864321; PubMed Central PMCID: PMCPMC5166504.
- [16] Stolz A, Ernst A, Dikic I. Cargo recognition and trafficking in selective autophagy. *Nat Cell Biol.* 2014 Jun;16(6):495–501. PubMed PMID: 24875736.
- [17] Tsuboyama K, Koyama-Honda I, Sakamaki Y, et al. The ATG conjugation systems are important for degradation of the inner autophagosomal membrane. *Science.* 2016 Nov 25;354(6315):1036–1041. PubMed PMID: 27885029.
- [18] Baksh S, Tommasi S, Fenton S, et al. The tumor suppressor RASSF1A and MAP-1 link death receptor signaling to Bax conformational change and cell death. *Mol Cell.* 2005 Jun 10;18(6):637–650. PubMed PMID: 15949439.
- [19] Tan KO, Fu NY, Sukumaran SK, et al. MAP-1 is a mitochondrial effector of Bax. *Proc Natl Acad Sci U S A.* 2005 Oct 11;102(41):14623–14628. PubMed PMID: 16199525; PubMed Central PMCID: PMCPMC1239892.
- [20] Tan KO, Tan KM, Chan SL, et al. MAP-1, a novel proapoptotic protein containing a BH3-like motif that associates with Bax through its Bcl-2 homology domains. *J Biol Chem.* 2001 Jan 26;276(4):2802–2807. PubMed PMID: 11060313.
- [21] Fu NY, Sukumaran SK, Yu VC. Inhibition of ubiquitin-mediated degradation of MOAP-1 by apoptotic stimuli promotes Bax function in mitochondria. *Proc Natl Acad Sci U S A.* 2007 Jun 12;104(24):10051–10056. PubMed PMID: 17535899; PubMed Central PMCID: PMCPMC1877986.
- [22] Huang NJ, Zhang L, Tang W, et al. The Trim39 ubiquitin ligase inhibits APC/CCdh1-mediated degradation of the Bax activator MOAP-1. *J Cell Biol.* 2012 Apr 30;197(3):361–367. PubMed PMID: 22529100; PubMed Central PMCID: PMCPMC3341153.
- [23] Lee SS, Fu NY, Sukumaran SK, et al. TRIM39 is a MOAP-1-binding protein that stabilizes MOAP-1 through inhibition of its poly-ubiquitination process. *Exp Cell Res.* 2009 Apr 15;315(7):1313–1325. PubMed PMID: 19100260.
- [24] Tan CT, Zhou QL, Su YC, et al. MOAP-1 mediates fas-induced apoptosis in liver by facilitating tBid recruitment to mitochondria. *Cell Rep.* 2016 Jun 28;16(1):174–185. PubMed PMID: 27320914.
- [25] Zaltsman Y, Shachnai L, Yivgi-Ohana N, et al. MTCH2/MIMP is a major facilitator of tBid recruitment to mitochondria. *Nat Cell Biol.* 2010 Jun;12(6):553–562. PubMed PMID: 20436477; PubMed Central PMCID: PMCPMC4070879.
- [26] Onodera J, Ohsumi Y. Autophagy is required for maintenance of amino acid levels and protein synthesis under nitrogen starvation. *J Biol Chem.* 2005 Sep 9;280(36):31582–31586. PubMed PMID: 16027116.
- [27] Kuma A, Hatano M, Matsui M, et al. The role of autophagy during the early neonatal starvation period. *Nature.* 2004 Dec 23;432(7020):1032–1036. PubMed PMID: 15525940.
- [28] Mizushima N, Levine B. Autophagy in mammalian development and differentiation. *Nat Cell Biol.* 2010 Sep;12(9):823–830. PubMed PMID: 20811354; PubMed Central PMCID: PMCPMC3127249.
- [29] Klionsky DJ, Abdelmohsen K, Abe A, et al. Guidelines for the use and interpretation of assays for monitoring autophagy (3rd edition). *Autophagy.* 2016;12(1):1–222. PubMed PMID: 26799652; PubMed Central PMCID: PMCPMC4835977.
- [30] Cann GM, Guignabert C, Ying L, et al. Developmental expression of LC3alpha and beta: absence of fibronectin or autophagy phenotype in LC3beta knockout mice. *Dev Dyn.* 2008 Jan;237(1):187–195. PubMed PMID: 18069693.
- [31] Zhang J, Wang J, Ng S, et al. Development of a novel method for quantification of autophagic protein degradation by AHA labeling. *Autophagy.* 2014 May;10(5):901–912. PubMed PMID: 24675368; PubMed Central PMCID: PMCPMC5119066.
- [32] Kaizuka T, Morishita H, Hama Y, et al. An autophagic flux probe that releases an internal control. *Mol Cell.* 2016 Nov 17;64(4):835–849. PubMed PMID: 27818143.
- [33] Kabeya Y, Mizushima N, Ueno T, et al. LC3, a mammalian homologue of yeast Apg8p, is localized in autophagosome

- membranes after processing. *Embo J.* **2000** Nov 1;19(21):5720–5728. PubMed PMID: 11060023; PubMed Central PMCID: PMC305793.
- [34] Takahashi Y, He H, Tang Z, et al. An autophagy assay reveals the ESCRT-III component CHMP2A as a regulator of phagophore closure. *Nat Commun.* **2018** Jul 20;9(1):2855. PubMed PMID: 30030437; PubMed Central PMCID: PMC6054611.
- [35] McEwan DG, Popovic D, Gubas A, et al. PLEKHM1 regulates autophagosome-lysosome fusion through HOPS complex and LC3/GABARAP proteins. *Mol Cell.* **2015** Jan 8;57(1):39–54. PubMed PMID: 25498145.
- [36] Ge L, Melville D, Zhang M, et al. The ER-Golgi intermediate compartment is a key membrane source for the LC3 lipidation step of autophagosome biogenesis. *Elife.* **2013** Aug;6(2):e00947. PubMed PMID: 23930225; PubMed Central PMCID: PMC3736544.
- [37] Bernard A, Popelka H, Klionsky DJ. A unique hairpin-type tail-anchored SNARE starts to solve a long-time puzzle. *Autophagy.* **2013** Jun 1;9(6):813–814. PubMed PMID: 23575358; PubMed Central PMCID: PMC3672291.
- [38] Itakura E, Kishi-Itakura C, Mizushima N. The hairpin-type tail-anchored SNARE syntaxin 17 targets to autophagosomes for fusion with endosomes/lysosomes. *Cell.* **2012** Dec 7;151(6):1256–1269. PubMed PMID: 23217709.
- [39] Kumar S, Jain A, Farzam F, et al. Mechanism of Stx17 recruitment to autophagosomes via IRGM and mammalian Atg8 proteins. *J Cell Biol.* **2018** Mar 5;217(3):997–1013. PubMed PMID: 29420192; PubMed Central PMCID: PMC5839791.
- [40] Maiuri MC, Zalckvar E, Kimchi A, et al. Self-eating and self-killing: crosstalk between autophagy and apoptosis. *Nat Rev Mol Cell Biol.* **2007** Sep 8;9(9):741–752. PubMed PMID: 17717517. DOI:10.1038/nrm2239.
- [41] Wei MC, Zong WX, Cheng EH, et al. Proapoptotic BAX and BAK: a requisite gateway to mitochondrial dysfunction and death. *Science.* **2001** Apr 27;292(5517):727–730. PubMed PMID: 11326099; PubMed Central PMCID: PMC3049805.
- [42] Germain M, Slack RSMCL-1. regulates the balance between autophagy and apoptosis. *Autophagy.* **2011** May;7(5):549–551. PubMed PMID: 21412051.
- [43] He C, The LB. BECN1 interactome. *Curr Opin Cell Biol.* **2010** Apr;22(2):140–149. PubMed PMID: 20097051; PubMed Central PMCID: PMC302854269.
- [44] Pattingre S, Tassa A, Qu X, et al. Bcl-2 antiapoptotic proteins inhibit BECN1-dependent autophagy. *Cell.* **2005** Sep 23;122(6):927–939. PubMed PMID: 16179260.
- [45] Kang R, Zeh HJ, Lotze MT, et al. The BECN1 network regulates autophagy and apoptosis. *Cell Death Differ.* **2011** Apr;18(4):571–580. PubMed PMID: 21311563; PubMed Central PMCID: PMC3131912.
- [46] Cuddeback SM, Yamaguchi H, Komatsu K, et al. Molecular cloning and characterization of Bif-1. A novel Src homology 3 domain-containing protein that associates with Bax. *J Biol Chem.* **2001** Jun 8;276(23):20559–20565. PubMed PMID: 11259440.
- [47] Takahashi Y, Coppola D, Matsushita N, et al. Bif-1 interacts with BECN1 through UVRAG and regulates autophagy and tumorigenesis. *Nat Cell Biol.* **2007** Oct 9;10(10):1142–1151. PubMed PMID: 17891140; PubMed Central PMCID: PMC2254521. DOI:10.1038/ncb1634.
- [48] Gillooly DJ, Morrow IC, Lindsay M, et al. Localization of phosphatidylinositol 3-phosphate in yeast and mammalian cells. *Embo J.* **2000** Sep 1;19(17):4577–4588. PMID: 10970851; PubMed Central PMCID: PMC302054.
- [49] Cong L, Ran FA, Cox D, et al. Multiplex genome engineering using CRISPR/Cas systems. *Science.* **2013** Feb 15;339(6121):819–823. PMID: 23287718; PubMed Central PMCID: PMC3795411.